

# Grindability of Dental Cast Ti-Zr Alloys

Masatoshi Takahashi, Masafumi Kikuchi and Osamu Okuno

Division of Dental Biomaterials, Tohoku University Graduate School of Dentistry, Sendai 980-8575, Japan

The purpose of this study was to improve the grindability of titanium by alloying with zirconium. The grindability of dental cast Ti-Zr alloys (10, 20, 30, 40 and 50 mass% Zr) was evaluated using a carborundum wheel. The Ti-Zr alloys up to 30 mass% Zr formed an  $\alpha$  structure, and the 40 mass% Zr and 50 mass% Zr alloys formed an  $\alpha'$  structure. The Ti-40 mass% Zr alloy at up to 1000 m/min and the Ti-50 mass% Zr alloy at up to 1250 m/min exhibited significantly higher grindability than titanium. More than twice the volume of metal was removed from the alloys than from titanium per minute. The improved grindability could be attributed to the  $\alpha'$  structure in addition to the decrease in elongation. The Ti-Zr alloys, which formed an  $\alpha'$  phase structure, are candidates for use as machinable biomaterial in dental applications.  
[doi:10.2320/matertrans.MRA2008403]

(Received October 27, 2008; Accepted January 13, 2009; Published February 25, 2009)

**Keywords:** biomaterial, titanium alloy, grindability, microstructure, dental alloy

## 1. Introduction

As a dental biomaterial, titanium has a reputation for offering excellent biocompatibility and corrosion resistance. However, it is considered one of the most difficult metals to machine (cut or grind).<sup>1)</sup> The poor machinability of titanium leads to a long processing time and short tool life.<sup>1)</sup> Therefore, improving the machinability of titanium will encourage practical dental applications of titanium. Furthermore, improved machinability may also promote the application of titanium using dental CAD/CAM.

We investigated the machinability of various experimental binary titanium alloys.<sup>2-6)</sup> The grindability of some Ti-Ag, Ti-Cu, and Ti-Nb alloys was superior to that of titanium.<sup>2,3)</sup> The common features of alloys with favorable grindability were not only a decreased elongation but also the existence of a secondary phase. For example, the Ti-Ag, Ti-Cu or Ti-Nb alloys precipitated a  $Ti_2Ag$ ,  $Ti_2Cu$  or  $\omega$  phase in the matrix, respectively. The precipitated secondary phase might work as a local brittle zone similar to the free-machining inclusions of free-machining materials.<sup>7)</sup> On the other hand, the grindability of Ti-Hf alloys that formed a single  $\alpha$  phase did not improve, although their elongation decreased.<sup>5)</sup>

Zirconium is known to show chemical and physical properties that are similar to titanium. According to the equilibrium phase diagram,<sup>8)</sup> the Ti-Zr system is an  $\alpha$ - $\beta$  isomorphous system, and there is no solubility limit for Zr in the titanium matrix. Zirconium improved the strength and hardness of titanium and decreased its elongation.<sup>9-15)</sup> Many studies have reported that Ti-Zr binary alloys showed superior corrosion resistance and biocompatibility when compared with titanium.<sup>16-19)</sup> Ho *et al.* investigated the grindability of Ti-Zr alloys up to 37 mass% Zr, which formed a single  $\alpha$  phase, and reported that the 37 mass% Zr alloy had better grindability than titanium at low speed<sup>14)</sup> (hereafter, mass% is expressed as %). The alloy phases of Ti-Zr alloys varied according to the compositions and cooling conditions.<sup>20,21)</sup> If the cooling rate from the  $\beta$ -region is fast enough, an acicular or lath-like martensite is formed. The martensite has a distorted hexagonal crystal lattice, similar to that of  $\alpha$ , and is referred to as  $\alpha'$ .<sup>22,23)</sup> The alloy phases for the Ti-Zr alloys have been reported to be as follows: for dental cast Ti-

Zr alloys with 39 to 85% Zr (25 to 75 mol% Zr), a martensitic structure  $\alpha'$ ,<sup>10)</sup> for quenched alloys with  $Zr \geq 30\%$ ,  $\alpha + \beta$ ;<sup>13,24)</sup> and for quenched 60% Zr (50 mol% Zr) alloys, a precipitated hexagonal crystal structure of the  $\omega$ .<sup>25)</sup> Phase transformations or the existence of secondary phases for the Ti-Zr alloys may drastically improve the grindability of titanium.

In the present study, the grindability of dental cast experimental Ti-Zr alloys up to 50% Zr was evaluated and compared with that of titanium. X-ray diffractometry (XRD) and microstructural observations of cast alloys were also performed to characterize the relationship between the grindability and the alloy phases.

## 2. Experimental Procedure

### 2.1 Preparation of specimens

Experimental binary titanium alloys with 10, 20, 30, 40 and 50% Zr were examined. Titanium was included as the control in this study. The desired amounts of titanium sponge (>99.8%, grade S-90, Sumitomo Titanium Corp., Amagasaki, Japan) and zirconium sponge (>99.6%, Toho Technical Service Co., Ltd, Chigasaki, Japan) were melted into one, 15 g button for each alloy in an argon-arc melting furnace (TAM-4S, Tachibana Riko, Sendai, Japan). Each button was melted six times and inverted five times to ensure alloy homogeneity.

Each alloy was cast into a plate pattern (3.5 mm  $\times$  8.5 mm  $\times$  30.5 mm) using a magnesia investment (Selevest CB, Selec, Osaka, Japan) in an argon gas-pressure dental casting machine (Castmatic-S, Iwatani, Osaka, Japan) at 200°C and then bench-cooled. Prior to testing, all the surfaces (approximately 250  $\mu$ m) of each casting were ground to remove the hardened surface layer, producing specimens measuring 3.0 mm  $\times$  8.0 mm  $\times$  30 mm. Three specimens were made for each metal.

### 2.2 X-ray diffractometry and microstructural observation

XRD was performed using Cu  $K\alpha$  radiation generated at 30 kV and 15 mA in an X-ray diffractometer (Miniflex CN2005, Rigaku, Tokyo, Japan). The peaks on the XRD

patterns were indexed using the powder diffraction file (PDF-2, JCPDS-ICDD 2004).

The specimen surfaces were polished and etched with an etching solution (1.0 ml HF, 4.0 ml HNO<sub>3</sub> and 300 ml H<sub>2</sub>O). The etched surfaces were observed using an optical microscope (PMG3-614U, Olympus, Tokyo, Japan).

### 2.3 Grinding test

A carborundum wheel [#4 (diameter 15.8 mm, thickness 1.6 mm), Shofu, Kyoto, Japan] placed on an electric dental handpiece (LM-I, GC, Tokyo, Japan) was used to grind the experimental metals as in previous studies.<sup>2-5)</sup> A 3.0 mm thick cross section of the specimens was ground for one minute at one of five circumferential speeds, i.e., 500, 750, 1000, 1250 or 1500 m/min, at 0.98 N.

Grindability was evaluated as the volume of metal removed per minute (grinding rate) and the volume ratio of metal removed compared to the wheel material lost (grinding ratio), which was calculated from its diameter loss. The grinding rate and the grinding ratio are related to the processing time and tool life, respectively. The test was performed twice for each specimen and grinding speed. A new wheel was employed for every test. The results ( $n = 6$ ) were statistically analyzed by one-way ANOVA and the Tukey HSD test at a significance level of  $\alpha = 0.05$ . After the grinding test, the metal chips, surfaces of the wheels, and ground surfaces of the metals were observed using a scanning electron microscope (JSM-6060, JEOL, Tokyo, Japan).

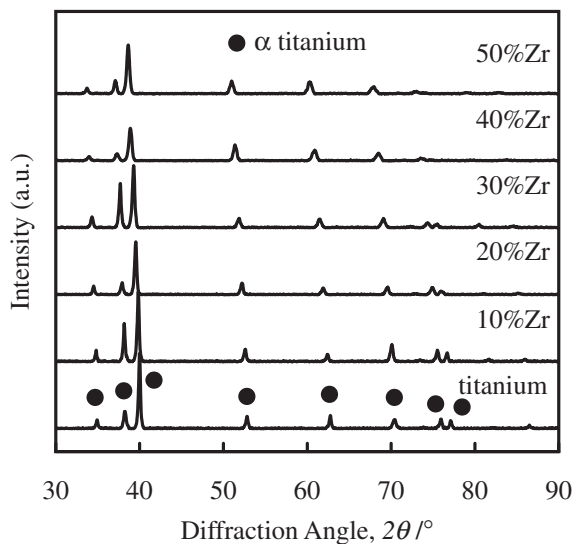


Fig. 1 X-ray diffraction patterns of Ti-Zr alloys.

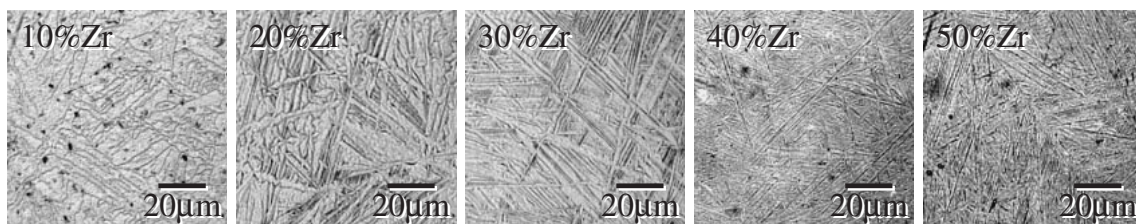


Fig. 2 Microstructures of etched Ti-Zr alloys.

### 2.4 Hardness test

Bulk hardness was determined by a Vickers microhardness tester (HM-102, Akashi, Yokohama, Japan) with a 1.961 N (200 gf) load and 30 s dwell time. Three randomly chosen points of each specimen were measured. The results were statistically analyzed by one-way ANOVA and the Tukey HSD test at a significance level of  $\alpha = 0.05$ .

## 3. Results

### 3.1 X-ray diffractometry and metallography

XRD patterns of the Ti-Zr alloys and titanium are displayed in Fig. 1. The peaks in the XRD pattern for titanium matched the diffraction angles of  $\alpha$  titanium well. With an increase in the Zr concentration, the peaks slightly shifted to the low angle side. There was no indication that the  $\beta$  phase or the  $\omega$  phase was included in any of the present diffraction patterns.

The microstructures of the etched Ti-Zr alloys are shown in Fig. 2. The microstructures of  $Zr \leq 30\%$  and  $Zr \geq 40\%$  were different. Coarse laths with a width of 1 to 3  $\mu\text{m}$  could be seen in the specimen of the Ti-Zr alloys with  $Zr \leq 30\%$ . Fine laths of about 500 nm could be seen in the 40% Zr and 50% Zr alloys.

### 3.2 Grindability

The grinding rates of the Ti-Zr alloys at five different grinding speeds are shown in Fig. 3. The grinding rates of the Ti-Zr alloys tended to increase as the concentration of Zr increased at 500 and 750 m/min. The rates for the alloys with  $Zr \geq 30\%$  were significantly higher ( $p < 0.05$ ) than that for titanium at the low speeds. At 1000 m/min or above, the rates for the alloys with  $Zr \leq 30\%$  were not higher than that for titanium. On the other hand, 40% Zr alloys at 1000 m/min and 50% Zr alloys at 1000 m/min and 1250 m/min exhibited significantly higher grinding rates ( $p < 0.05$ ) than titanium. The rates of the alloys were more than twice that of titanium.

The grinding ratios of the Ti-Zr alloys at five different grinding speeds are shown in Fig. 4. The grinding ratios of the Ti-Zr alloys had large standard deviations, and no significant difference with titanium was found in any composition or grinding speed ( $p > 0.05$ ).

### 3.3 Observation of metal chips, wheels, and ground surfaces after grinding

Typical metal chips that resulted from grinding are shown in Fig. 5. Although no quantitative analysis was performed, the size of the metal chips of the Ti-Zr alloys with  $Zr \leq 30\%$

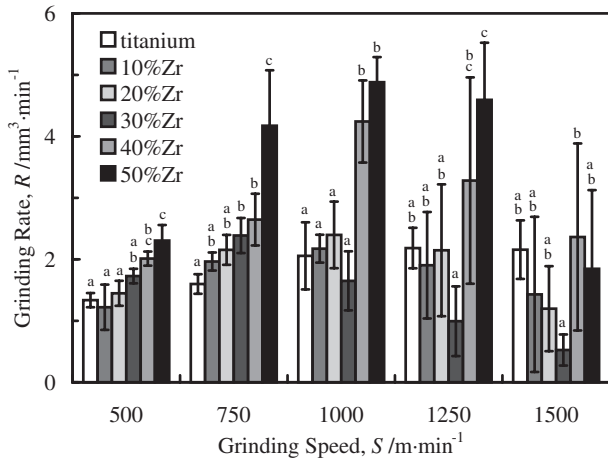


Fig. 3 Grinding rate of Ti-Zr alloys. Identical letters indicate no statistical differences among each grinding speed ( $p > 0.05$ ).

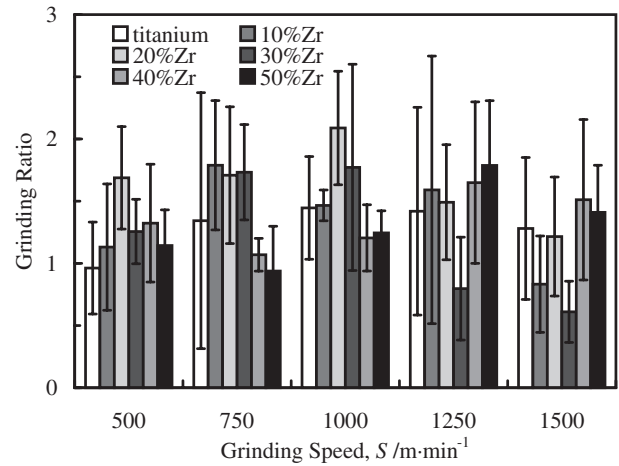


Fig. 4 Grinding ratio of Ti-Zr alloys.

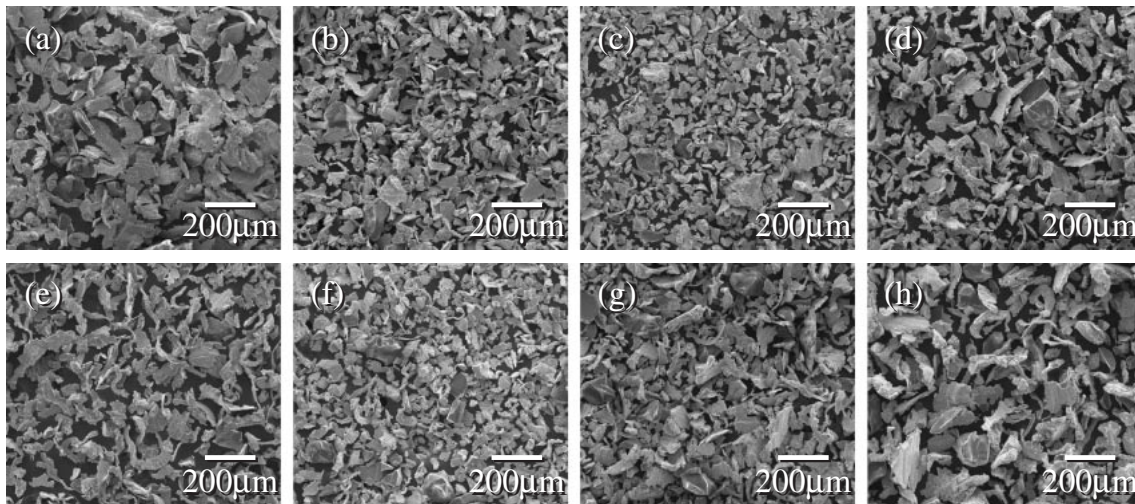


Fig. 5 Metal chips resulting from grinding: (a) titanium, (b) 30% Zr, (c) 40% Zr and (d) 50% Zr at 500 m/min; and (e) titanium, (f) 30% Zr, (g) 40% Zr and (h) 50% Zr at 1000 m/min.

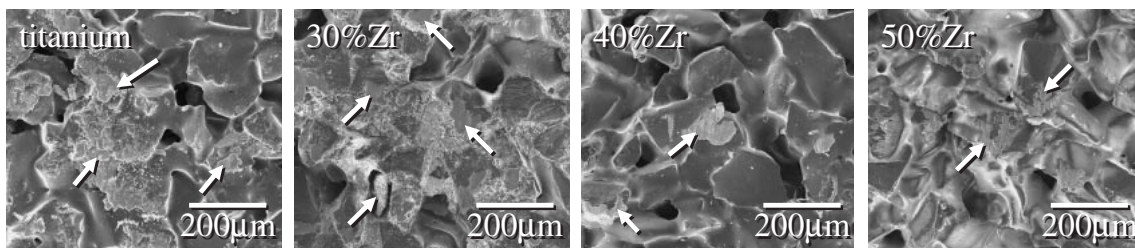


Fig. 6 Wheel surfaces after grinding. The arrow indicates the adhered metals.

(80 to 150  $\mu\text{m}$  in length) generally appeared to be somewhat smaller than that of the chips of titanium (150 to 200  $\mu\text{m}$  in length). The size of the metal chips of the alloys with  $\text{Zr} \geq 40\%$  varied. Larger metal chips (approximately 200  $\mu\text{m}$  in length), on the whole, were observed more frequently for these alloys.

Wheel surfaces after the grinding test at 1000 m/min are shown in Fig. 6. The adhesion of metal to the wheel surfaces was observed in a large area of the wheels used for titanium and the alloys with  $\text{Zr} \leq 30\%$  at high grinding

speeds and the 40% Zr and 50% Zr alloys at the 1500 m/min. A grinding burn (discoloration of the surface caused by the heat of grinding)<sup>7)</sup> was found on the ground surfaces of these alloys. On the other hand, adhesion of metal was observed partly in the wheel used for the 40% Zr and 50% Zr alloys at 1000 and 1250 m/min, and a grinding burn was not observed on the ground surfaces of these alloys. No clear difference was noted in the appearance of the wheel and the ground surface among the Ti-Zr alloys and titanium at low grinding speeds.

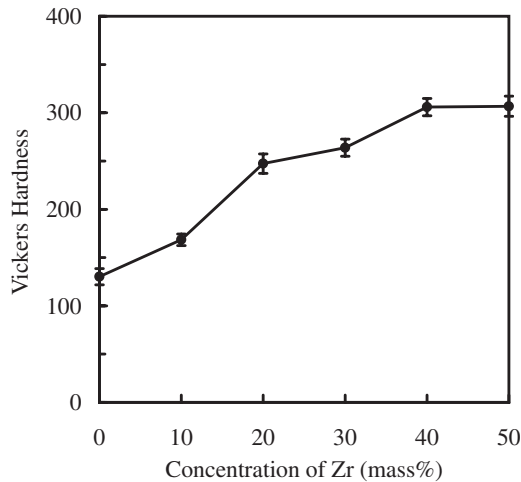


Fig. 7 Hardness of Ti-Zr alloys.

### 3.4 Hardness

The results of the hardness test for the Ti-Zr alloys are shown in Fig. 7. The hardness of the Ti-Zr alloys increased as the concentration of the Zr increased, and it was significantly higher ( $p < 0.05$ ) than that of titanium.

## 4. Discussion

### 4.1 Alloy phases

The XRD peaks for Ti-Zr alloys resembled the peaks for  $\alpha$  titanium. It is difficult to identify the differences between  $\alpha'$  and  $\alpha$  by XRD because the crystal structure of  $\alpha'$  is a slightly deformed crystal structure of  $\alpha$ , and  $\alpha'$  shows almost the same XRD peaks as  $\alpha$ . Therefore, the phases in this study were determined by microstructural observations, as in previous studies.<sup>9,10,12,13</sup> The microstructures in the Ti-Zr alloy with  $Zr \leq 30\%$  resembled the typical acicular structure of  $\alpha$  titanium.<sup>22,23</sup> On the other hand, the fine martensitic laths in the Ti-Zr alloy with  $Zr \geq 40\%$  closely resembled the martensite microstructures of  $\alpha'$ , which had been shown by E. Kobayashi *et al.*<sup>10</sup> and S. Kobayashi *et al.*<sup>26</sup> Judging from the microstructures, the alloy phase of  $Zr \leq 30\%$  was the  $\alpha$  phase, and the phase of  $Zr \geq 40\%$  was the  $\alpha'$  phase.

### 4.2 Mechanical properties

The Ti-Zr alloys became harder than that of titanium as the concentration of Zr increased. The increased hardness was caused by solid-solution hardening. The hardness of the alloys in this study was similar to that in previous studies.<sup>10–12</sup> Many studies have reported on the mechanical properties of Ti-Zr alloys.<sup>9–15</sup> Thus, we assume that the other mechanical properties were also similar to those in previous studies.

### 4.3 Grinding rates of Ti-Zr alloys with $Zr \leq 30\%$

One approach to improving machinability is to reduce the ductility of an alloy.<sup>27,28</sup> The elongation of Ti-Zr alloys became lower than that of titanium as the concentration of Zr increased.<sup>11–13</sup> The grinding rates of the Ti-Zr alloys increased at low speed as the concentration of Zr increased, in other words, as their elongation decreased, and the rates of

the 30% Zr alloy were significantly higher than those of titanium. These results were similar to those found by Ho *et al.*<sup>14</sup> The alloy with higher grinding rates produced smaller metal chips than that of titanium (Fig. 4), as in previous studies.<sup>2,3</sup>

Despite the finer metal chips, the grinding rates of the Ti-Zr alloy with  $Zr \leq 30\%$  tended to decrease at 1000 m/min or above. A decrease in the rate of metal chip formation (grinding rate) resulted in overheating and a grinding burn on the ground surfaces because the majority of the grinding heat is carried away with the metal chips. The reason for the decreased grinding rate was the occurrence of adhesion of metal on the wheel surface. The adhesion caused filling of the pores of the grinding wheel (loading) and obstructed self-dressing of the wheel.<sup>7</sup> Similar results were found for Ti-Au alloys.<sup>4</sup>

### 4.4 Grinding rates of Ti-Zr alloys with $Zr \geq 40\%$

The grinding rates of the alloys with  $Zr \geq 40\%$  increased drastically at 1000 m/min or above. In contrast to the Ti-Zr alloys with  $Zr \leq 30\%$ , adhesion of metal was seldom observed on the wheel used for the 40% Zr and 50% Zr alloys, and self-dressing of the wheel was not obstructed. Because the 40% Zr and 50% Zr alloys were harder and stronger than the 30% Zr alloy,<sup>9–11</sup> 40% Zr and 50% Zr would not work as well as 30% Zr for grinding. Although reduced elongation of the alloy helps improve machinability,<sup>27,28</sup> the elongation did not decrease significantly from the 30% Zr to the 50% Zr alloy.<sup>9–11</sup> Unlike the cases of Ti-Ag or Ti-Cu alloys with better grindability, the metal chips of the 40% Zr and 50% Zr alloys were not smaller than those of titanium (Fig. 4). Therefore, the abrupt increase in the grinding rate of the Ti-Zr alloys from  $Zr \leq 30\%$  to  $Zr \geq 40\%$  at high speed cannot be explained by their reduced elongation alone. One explanation for the abrupt increase could be a microstructural change because the  $\alpha$  phase ( $Zr \leq 30\%$ ) changed to an  $\alpha'$  phase ( $Zr \geq 40\%$ ). The alloy phase of 37% Zr alloy by Ho *et al.* was a single  $\alpha$  phase, and the grinding rates of the 37% Zr did not increase at high grinding speeds.<sup>14</sup> On the other hand, the alloy phase of the 40% Zr alloy in our study was the  $\alpha'$  phase, and the grinding rates increased significantly at high speeds. The strain rate and temperature differed between the grinding test and the tensile test. The  $\alpha'$  phase in the Ti-Zr alloys might show different mechanical properties at a grinding test and a tensile test. At the 1500 m/min, the rates of the alloys with  $Zr \geq 40\%$  were similar to that of titanium, and a grinding burn was found on the alloys. The grinding speed of 1500 m/min was apparently too fast to grind the alloys.

### 4.5 Grinding ratios of Ti-Zr alloys

Although the mean values of the grinding ratios of some Ti-Zr alloys were higher than those of titanium, no significant difference between the Ti-Zr alloys and titanium was found with any composition or grinding speed because the ratios had large standard deviations. On the other hand, Ho *et al.*<sup>14</sup> found a significant difference in the grinding ratios in some compositions or grinding speeds despite achieving large standard deviations similar to those in our results. A discrepancy in the results could probably be attributed to a

difference in the statistical procedures. Duncan's multiple comparison test, which was used by Ho *et al.*, has high type I error rates and occasionally finds a statistically significant difference when no significant difference actually exists.<sup>29)</sup> Many statisticians have said that Duncan's test cannot be recommended.<sup>30,31)</sup>

Because no significant difference was found in the grinding ratio between the experimental Ti-Zr alloys and titanium, the addition of Zr to titanium did not help improve tool life. However, the addition of Zr helped improve processing time because the grinding rates of the Ti-Zr alloys were significantly higher than those of titanium. Therefore, Ti-Zr alloys, especially Zr  $\geq$  40%, had excellent grindability.

## 5. Conclusion

Dental cast Ti-Zr alloys with 40% Zr and 50% Zr formed an  $\alpha'$  structure. The Ti-40%Zr alloy at up to 1000 m/min and the Ti-50%Zr alloy at up to 1250 m/min exhibited significantly higher grindability than titanium. The improved grindability could be attributed to the  $\alpha'$  structure in addition to the decrease in elongation. Ti-Zr alloys, which formed an  $\alpha'$  phase structure, are candidates for use as machinable biomaterial in dental applications.

## Acknowledgments

The authors gratefully acknowledge Sumitomo Titanium Corporation for supplying the high-purity titanium sponge.

## Appendix

A preliminary report on this study was presented at the 85th General Session & Exhibition of the International Association for Dental Research on March 2007.

## REFERENCES

- 1) A. R. Machado and J. Wallbank: Proc. Inst. Mech. Eng. Part B **204** (1990) 53–60.
- 2) M. Kikuchi, M. Takahashi, T. Okabe and O. Okuno: Dent. Mater. J. **22** (2003) 191–205.
- 3) M. Kikuchi, M. Takahashi and O. Okuno: Dent. Mater. J. **22** (2003) 328–342.
- 4) M. Takahashi, M. Kikuchi and O. Okuno: Dent. Mater. J. **23** (2004) 203–210.
- 5) M. Kikuchi, M. Takahashi, H. Sato, O. Okuno, M. Nunn and T. Okabe: J. Biomed. Mater. Res. B **77** (2006) 34–38.
- 6) M. Kikuchi, M. Takahashi and O. Okuno: Dent. Mater. J. **27** (2008) 216–220.
- 7) J. R. Davis: *ASM materials engineering dictionary*, (ASM International, Materials Park, 1992) pp. 127–256.
- 8) J. L. Murray: *Phase diagrams of binary titanium alloys*, (ASM International, Metals Park, 1987) pp. 340–345.
- 9) E. Kobayashi, H. Doi, T. Yoneyama, H. Hamanaka, S. Matsumoto and K. Kudaka: J. J. Dent. Mater. **14** (1995) 321–328.
- 10) E. Kobayashi, S. Matsumoto, H. Doi, T. Yoneyama and H. Hamanaka: J. Biomed. Mater. Res. **29** (1995) 943–950.
- 11) Y. Etchu, M. Okazaki, H. Noguchi and E. Masuhara: J. J. Dent. Mater. **11** (1992) 270–271.
- 12) O. Okuno, A. Shimizu and I. Miura: J. J. Dent. Mater. **4** (1985) 708–715.
- 13) A. G. Imgram, D. N. Williams and H. R. Ogden: J. Less-Common Metals. **4** (1962) 217–225.
- 14) W. F. Ho, W. K. Chen, S. C. Wu and H. C. Hsu: J. Mater. Sci. Mater. Med. **19** (2008) 3179–3186.
- 15) M. Takahashi, E. Kobayashi, H. Doi, T. Yoneyama and H. Hamanaka: J. Japan Inst. Metals **64** (2000) 1120–1126.
- 16) T. Tsuchiya, A. Nakamura, Y. Ohshima, E. Kobayashi, H. Doi, T. Yoneyama and H. Hamanaka: Tissue Eng. **4** (1998) 197–204.
- 17) S. Y. Yu, J. R. Scully and C. M. Vitus: J. Electrochem. Soc. **148** (2001) 68–78.
- 18) N. T. C. Oliveira, S. R. Biaggio, R. C. Rocha-Filho and N. Bocchi: J. Biomed. Mater. Res. A **74** (2005) 397–407.
- 19) Y. Ikarashi, K. Toyoda, E. Kobayashi, H. Doi, T. Yoneyama, H. Hamanaka and T. Tsuchiya: Mater. Trans. **46** (2005) 2260–2267.
- 20) Y. C. Huang, S. Suzuki, H. Kaneko and T. Sato: Proc. Int. Conf., ed. by R. I. Jaffee, (Sci. Technol. Appl. Titanium, 1970) pp. 691–693.
- 21) Y. C. Huang, S. Suzuki, H. Kaneko and T. Sato: Proc. Int. Conf., ed. by R. I. Jaffee, (Sci. Technol. Appl. Titanium, 1970) pp. 695–698.
- 22) G. F. Vander Voort: *ASM handbook, volume 9 metallography and microstructures*, (ASM International, Materials Park, 2004) pp. 899–917.
- 23) R. Boyer, G. Welsch and E. W. Collings: *Materials properties handbook: titanium alloys*, (ASM International, Materials Park, 1994) pp. 1051–1060.
- 24) P. Duwez: J. Inst. Met. **80** (1952) 525–527.
- 25) B. A. Hatt, J. A. Roberts and G. I. Williams: Nature **180** (1957) 1406.
- 26) S. Kobayashi, K. Nakai and Y. Ohmori: Mater. Trans. **42** (2001) 2398–2405.
- 27) T. Okabe, M. Kikuchi, C. Ohkubo, M. Koike, O. Okuno and Y. Oda: JOM J. Miner. Met. Mater. Soc. **56** (2004) 46–48.
- 28) K. S. Chan, M. Koike and T. Okabe: Metall. Mater. Trans. A **37** (2006) 1323–1331.
- 29) J. L. Gill: J. Dairy Sci. **64** (1981) 1494–1519.
- 30) J. W. Tukey: Statist. Sci. **6** (1991) 100–116.
- 31) J. C. Hsu: *Multiple comparisons theory and methods*, (Chapman & Hall, London, 1996) pp. 119–144.